IEEE Access
Multidisciplinary | Rapid Review | Open Access Journal

Received August 11, 2019, accepted August 24, 2019, date of publication August 28, 2019, date of current version September 12, 2019.

Digital Object Identifier 10.1109/ACCESS.2019.2938067

Neuroadaptive Distributed Output Feedback Tracking Control for Multiple Marine Surface Vessels With Input and Output Constraints

GUOQING XIA, CHUANG SUN, BO ZHAO, XIAOMING XIA, AND XIANXIN SUN
College of Automation, Harbin Engineering University, Harbin 150001, China

Corresponding author: Chuang Sun (sunchuang@hrbeu.edu.cn)

This work was supported in part by the 7th Generation Ultra Deep Water Drilling Unit Innovation Project, and in part by the National Natural Science Foundation of China through the research on green and safe mooring-assisted dynamic positioning technology for all-weather deepwater platform under Grant 51879049.

ABSTRACT In this paper, a neuroadaptive distributed output feedback formation tracking control scheme for multiple marine surface vessels with model uncertainties, unknown environmental disturbances and input and output constraints is proposed. A neural network based observer is developed to reconstruct the unmeasured velocity and approach the model uncertainties. To handle the input constraint, an auxiliary dynamic system is introduced. The tracking error transformation and the barrier Lyapunov function are used to tackle with the output constraint. Subsequently, by using the estimated velocity of neighboring vessels, neuroadaptive distributed output feedback controllers are developed. Furthermore, to avoid directly taking the time derivation of virtual control law and generate smooth reference signals, linear tracking differentiators are employed. Finally, it is shown that all the signals in the closed-loop system are bounded via Lyapunov analysis. Simulations are carried out to verify the proposed control scheme.

INDEX TERMS Barrier Lyapunov function, distributed control, input constraint, marine surface vessels, output constraint, output feedback control.

I. INTRODUCTION

In recent years, distributed control for multiple marine surface vessels (MSVs) has gained much attention, since a formation of MSVs working together can accomplish more challenging missions than a single MSV, such as surveillance, reconnaissance, rescue operations, dynamic guarding, and mobile nodes of sensor network [1], [2]. Maintaining a relative formation is usually required when MSVs perform corresponding missions.

In most cases, in addition to vessel position, velocity is also required for controller design. The position-heading information for MSV is easily available using global satellite navigation system and gyro, but the velocity may not be measured. Therefore, it is necessary to investigate distributed control problem in the absence of velocity measurements. Some output feedback controllers were proposed without using velocity measurement in [3]–[5]. Reference [3] proposed the passive nonlinear observer for MSV, where the velocity and low-frequency motion of vessel can be reconstructed. A hub motion estimation algorithm using sensor fusion of a global navigation satellite system and an inertial measurement unit was designed in [4]. In [5], an observer backstepping technique was used to design for multiple MSVs maneuvering operation. These methods assume that the model parameters of the system are known.

However, the parameters of a MSV can hardly be known accurately, and the hydrodynamic parameters of MSVs are time-varying in general. Thus, to adapt the model uncertainties of MSVs' is need to be considered in controller design. Neural network (NN) has the excellent approximation and learning performance, and has became the powerful and popular tools to estimate the model uncertainties in nonlinear system [6]–[8]. Some NN based output feedback controllers were designed in [9]–[11]. In [9], an adaptive NN controller was presented, where a high-gain observer was used to reconstruct the unmeasurable velocity. In [10], a neural adaptive output feedback tracking controller was developed using a linear observer. The linear observer was used to update the NN parameters. A NN based predictor

The associate editor coordinating the review of this article and approving it for publication was Jun Hu.

was designed to recover unmeasured velocity information in [11]. But an auxiliary variable was needed to reconstruct the velocity.

Input saturation constraint may severely degrade the control performance and lead to instability. For multiple MSV's distributed control system, it may affect the cooperative control performance since the control forces and moment that can be calculated by controller may exceed the maximum forces and moment produced by MSV's thrusters. The input constraint problem of various system has gained much attention. In [13], an adaptive control of single input uncertain nonlinear systems was proposed in the presence of input saturation and unknown external disturbance, where input saturation was handled by using a Nussbaum function. In [14], adaptive tracking control algorithms were proposed for a class of uncertain multi-input and multi-output nonlinear systems with non-symmetric input constraints, where an auxiliary system was designed to handle the input saturation. For multiple MSVs system, [16] proposed a cooperative control methods of multiple dynamic positioning vessels subject to unknown time-varying environmental disturbances and input saturation. Reference [15] considered a cooperative path following control for multiple MSVs subjected to unstructured disturbances, unknown dynamical uncertainty and input saturation, where the auxiliary system was as same as [14]. From the vessels' work mode, it is necessary to account for input saturation for multiple MSVs.

Besides input constraint, another challenge to distributed control for multiple MSVs is output (position) constraint. This is a common requirement in marine operations, such as collision avoidance, sea-bed scanning, and etc. Early research on the constrained formation control problem was [17], where a successful coordination strategy was proposed based on a constraint function. In addition, approaches based on model predictive control were used to the formation control of multi-agent in [18] and [19]. However, these model predictive control based methods introduce heavy computational load, which restricts application to formation control with a large number of agents. In [20], a resilient algorithm based on receding-horizon technique was proposed with states and input constraints. In [21]–[24], containment control of multi-agent systems in the presence of multiple leaders was proposed, where agents were converge to a geometric space spanned by multiple leaders without output constraint for each vessel. In addition, the barrier Lyapunov function (BLF) method is another approach to deal with the output constraint which can avoid the necessity of explicit solutions [25]. This method has been extended to handle single MSV [26]–[28] and multi-agent systems [29] and [30] with output constraint.

In this paper, we consider the formation tracking problem of multiple MSVs problem with model uncertainties, unknown time-varying environmental disturbances, and input and output constraints. A neuroadaptive distributed output feedback control scheme is proposed. The MSVs are interconnected through a directed communication network. In order to reconstruct the unmeasured velocity information as well as to identify the unknown model dynamics, a NN based observer is developed for each vessel. An auxiliary dynamic system is introduced to handle the input saturation. Two generated states of auxiliary dynamics system are used in controller designing process, which can improve the control performance in case of input constraint. The tracking error transformation and BLF are used to deal with output constraint. Then, based on the estimated velocity, auxiliary states and BLF, a kinematic control law is proposed. Besides, a linear tracking differentiator (LTD) is employed to generate smooth reference signal, which also can avoid directly taking the time derivation of kinematic control law. Finally, a NN based kinetic control law for each vessel is constructed. It is proved that all signals in the closed-loop control system are bounded.

The main contributions of this paper are summarized as follows. First, compared with the designed observers in [9], [12] and [27], the unknown model dynamics and unmeasured velocity can be simultaneously estimated by the proposed NN based observer. Second, unlike the existing work [11], [17] and [22] ignoring the input and output constraints, in this paper, auxiliary dynamic systems and BLFs are employed to handle the constraints. Third, LTDs are introduced to avoid directly taking the time derivation of kinematic control law, and reduce the effect of system noise in contrast to the dynamic surface control (DSC) in [16] and [35].

This paper is organized as follows. Section II gives some necessary preliminaries and the problem formulation. Section III proposes designs the distributed output feedback controller and gives the stability analysis. Section IV gives simulations. Section V concludes this paper.

II. PRELIMINARIES AND PROBLEM FORMATION

A. NOTATION

The following notations will be used throughout this paper. $|\cdot|$ represents the absolute value of a scalar. $\lambda_{\min}(\cdot)$ and $\lambda_{\max}(\cdot)$ represents minimum and maximum eigenvalue of a square matrix, respectively. $\|\cdot\|$ represents the Euclidean norm. $||\cdot||_F$ represents Frobenius norm. $\mathbb{R}^{m\times m}$ represents the $m\times m$ dimensional Euclidean Space. diag$\{a_j\}$ represents a block-diagonal matrix with a_j being the jth diagonal element. $(\cdot)^T$ and $(\cdot)^{-1}$ denote the transpose and inverse of a matrix, respectively. $\otimes$ represents the Kronecker product of matrices. tr$(\cdot)$ represents the trace of the respective matrix. Throughout the paper, i is used as the index of the MSVs, i.e. $i = 1, \ldots, n$.

B. GRAPH THEORY

The graph theory will be used to describe the communication topology of n MSVs. A directed graph $\mathcal{G} = \{\mathcal{V}_\mathcal{G}, \mathcal{E}\}$ consists of a vertex set $\mathcal{V}_\mathcal{G} = \{1, 2, \ldots, n\}$ and an edge set $\mathcal{E} = \{(i,j) \in \mathcal{V}_\mathcal{G} \times \mathcal{V}_\mathcal{G}\}$. $(i,j) \in \mathcal{E}$ describes that the information of vessel i is available to vessel j, and we say vessel i is a neighbor of vessel j. The neighbors of vessel i is described by $\mathcal{N}_i = \{j \in \mathcal{V}_\mathcal{G}, (i,j) \in \mathcal{E}\}$. Define an adjacency matrix $\mathcal{A} = [a_{ij}] \in \mathbb{R}^{n\times n}$, where $a_{ij} = 1$, if $(i,j) \in \mathcal{E}$; otherwise

$a_{ij} = 0$. If $a_{ij} = a_{ji}$, the graph is undirected; otherwise is directed. The Laplacian matrix $\mathcal{L}$ associates with the graph $\mathcal{G}$ is defined as $\mathcal{L} = \mathcal{D} - \mathcal{A}$, where $\mathcal{D} = \text{diag}\{d_1, \ldots, d_n\}$ with $d_i = \sum_{j=1}^{n} a_{ij}$. A diagonal matrix $\mathcal{A}_0 = \text{diag}\{a_{i0}\}$ is defined to be a leader adjacency matrix, where $a_{i0} = 1$, if and only if the ith vessel has access to the information of leader vessel, $a_{i0} = 0$, if not the case. Finally the information exchange matrix is defined as $\mathcal{H} = \mathcal{L} + \mathcal{A}_0$.

In this paper, a reference signal $\eta_d \in \mathbb{R}^3$ is viewed as a virtual leader (indexed by n+1), the communication between the n vessels and the leader can be described as an augmented graph $\bar{\mathcal{G}} = \{\bar{\mathcal{V}}_{\bar{\mathcal{G}}}, \bar{\mathcal{E}}\}$ with n+1 nodes, where $\bar{\mathcal{V}}_{\bar{\mathcal{G}}} = \{1, \ldots, n+1\}$ and $\bar{\mathcal{E}} = \{(i,j) \in \bar{\mathcal{V}}_{\bar{\mathcal{G}}} \times \bar{\mathcal{V}}_{\bar{\mathcal{G}}}\}$. Then the following assumption is made.

Assumption 1: There exists at least one directed path from the leader to every other vessel in the graph.

C. NEURAL NETWORK

In this paper, a radial basis function NN (RBFNN), which consisting an input layer, a hidden layer with a nonlinear radial basis function activation function and a output layer, is used as an approximator to estimate model uncertainties and environmental disturbances. Given a positive number $\bar{\varepsilon}$ and a continuous function $f(\varsigma) : \mathbb{R}^n \to \mathbb{R}^k$ can be approximated by an RBFNN as [31]

$$f(\varsigma) = W^T h_j(\varsigma) + \varepsilon(\varsigma), \forall \varsigma \in \Omega_\varsigma, \quad j = 1, 2 \ldots, m, \quad (1)$$

where $\varepsilon(\varsigma) \in \mathbb{R}^k$ is the estimation error satisfying $\|\varepsilon(\varsigma)\| \leq \bar{\varepsilon}$. ς is the input vector, m is the number of hidden-layer neurons, $W \in \mathbb{R}^{m \times k}$ is the hidden-layer-to-output interconnection weights and bounded by $\|W\|_F \leq W^*$ with W^* being a positive constant, $h_j(\varsigma) \in \mathbb{R}^m$ is the vector of neurons basis function which is bounded, i.e. $||h_j|| \leq \bar{h}$, where $\bar{h}$ is positive constant. In general, $h_j(\varsigma)$ is chosen as the Gaussian function, which has the form as

$$h_j(\varsigma) = \exp\left[-\frac{\|\varsigma - c_j\|^2}{b_j^2}\right], \quad (2)$$

where $c_j \in \mathbb{R}^n$ and $b_j > 0$ is the center and width of the jth kernel unit, respectively.

In general, the optimal weight vector W is unknown and need to be estimated in the controller design. Let $\hat{W}$ be the estimation of W, and define the weight estimation error as $\tilde{W} = \hat{W} - W$. The optimal weight vector W is chosen as the value of $\hat{W}$ that minimize $\varepsilon(\varsigma)$, and define $W = \arg \min_{\hat{W} \in \mathbb{R}^{n \times m}} \{\sup_{\varsigma \in \Omega_\varsigma} |f(\varsigma) - \hat{W}^T h_j(\varsigma)|\}$.

D. MATHEMATICAL PRELIMINARIES

To deal with the output constraint, a BLF is introduced as

$$V = \frac{1}{2} \ln \frac{k^2}{k^2 - z^2}, \quad (3)$$

where $|z| \leq k$ with $k > 0$. Then, the following lemma hold.

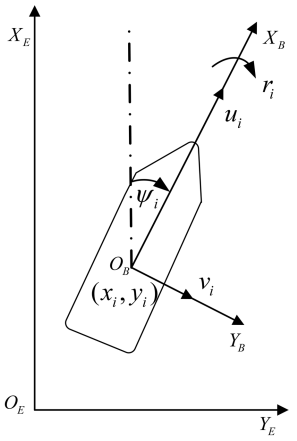

FIGURE 1. Earth-fixed frame and body-fixed frame.

Lemma 1 [25]: For any constant $k \in \mathbb{R}$, when $|z| < k$, the following inequality is held.

$$\ln \frac{k^2}{k^2 - z^2} < \frac{z^2}{k^2 - z^2}. \quad (4)$$

E. PROBLEM FORMATION

Consider a networked of n MSVs, labeled as 1 to n. Let $\eta_i = [x_i, y_i, \psi_i]^T \in \mathbb{R}^3$ denote the position and yaw angle vector expressed in earth fixed frame $X_E O_E Y_E$ as shown in Figure 1. Let $\upsilon_i = [u_i, v_i, r_i]^T \in \mathbb{R}^3$ denote the velocity and yaw rate vector expressed in the body fixed frame $X_B O_B Y_B$. Then, the three degrees of freedom horizontal motion mathematical model for the ith marine surface vessel is given as [32]

$$\dot{\eta}_i = R(\psi_i)\upsilon_i, \quad (5)$$

$$M_i \dot{\upsilon}_i = -D_i(\upsilon_i)\upsilon_i - C_i(\upsilon_i)\upsilon_i + \tau_i + \tau_{iw}, \quad (6)$$

where $M_i = M_i^T \in \mathbb{R}^{3\times3}$ denotes the MSV inertia matrix. $C_i(\upsilon_i) = -C_i^T(\upsilon_i) \in \mathbb{R}^{3\times3}$ represents a skew-symmetric matrix of Coriolis and centripetal term. $D_i(\upsilon_i) \in \mathbb{R}^{3\times3}$ is a nonlinear damping matrix. $\tau_{iw} = [\tau_{iw1}, \tau_{iw2}, \tau_{iw3}]^T$ denotes the environmental disturbances vector, which is caused by wind, waves, ocean currents in surge, sway and yaw, respectively. $R_i(\psi_i)$ is the rotation matrix. It satisfies $\|R(\psi_i)\| = 1$ and $R^T(\psi_i)R(\psi_i) = I_{3\times3}$, and its time derivative is $\dot{R}(\psi_i) = r_i R(\psi_i) S$, where

$$R(\psi_i) = \begin{bmatrix} \cos(\psi_i) & -\sin(\psi_i) & 0 \\ \sin(\psi_i) & \cos(\psi_i) & 0 \\ 0 & 0 & 1 \end{bmatrix}, \quad S = \begin{bmatrix} 0 & -1 & 0 \\ 1 & 0 & 0 \\ 0 & 0 & 0 \end{bmatrix}. \quad (7)$$

To facilitate the following text, we omit ψ_i without confusion, i.e. $R_i = R(\psi_i)$, $\dot{R}_i = \dot{R}(\psi_i)$ and $R_i^T = R^T(\psi_i)$. $\tau_i \in \mathbb{R}^3$ denotes the control forces and moment with constraint as

$$\tau_i = \begin{cases} \tau_{i\max}, & \text{if } \tau_{ic} > \tau_{i\max} \\ \tau_{ic}, & \text{if } \tau_{i\min} \leq \tau_{ic} \leq \tau_{i\max} \\ \tau_{i\min}, & \text{if } \tau_{ic} < \tau_{i\min} \end{cases}, \quad (8)$$

where $\tau_{i\max} \in \mathbb{R}^3$ and $\tau_{i\min} \in \mathbb{R}^3$ are the maximum and minimum control forces and moment produced by the thruster. $\tau_{ic} = [\tau_{ic1}, \tau_{ic2}, \tau_{ic3}]^T$ is calculated by the distributed controller.

The *control objective* of this paper is to design a distributed output feedback controller for each MSV to track reference signal η_d with model uncertainties, input constraint and only using the position measurement η_i. Specifically, it is to achieve the following two objectives.

1) Force MSVs maintain a desired formation and track the reference signal η_d.

$$\lim_{t\to\infty} \|\eta_i - \eta_d - \vartheta_i\| \le o_i, \tag{9}$$

where $\vartheta_i \in \Re^3$ is the desired relative deviation between the vessel i and η_d, and o_i is a positive constant which can be made small enough by choosing the control parameters.

2) The position for each MSV remains in the set $\Omega_{\eta_i} = \{|\eta_i - \vartheta_i| < k_{ic}\}$, where k_{ic} is specified later.

Before designing, the following assumptions are made.

Assumption 2 [16]: The time-varying environmental disturbances τ_{iw} is bounded, i.e. $|\tau_{iw}| \le \bar{\tau}_{iw}$ where $\bar{\tau}_{iw}$ is positive constant.

Assumption 3: The reference signal η_d and $\dot{\eta}_d$ are bounded.

III. DISTRIBUTED CONTROLLER DESIGN FOR MSVS

A. OBSERVER DESIGN

In practice, the parameters M_i, D_i and C_i are difficult to be determined, the ship model often includes uncertainties and unmodeled dynamics. To design the observer, the system model (5) and (6) is rewritten as

$$\dot{\eta}_i = R_i \upsilon_i, \tag{10}$$

$$\bar{M}_i\, \dot{\upsilon}_i = \tau_i - f_i(\upsilon_i), \tag{11}$$

where $\bar{M}_i^T = \bar{M}_i$ is the nominal inertial matrix being positive definite, and $f_i(\upsilon_i) = (I_{3\times3} - \bar{M}_i M_i^{-1})\tau_i + \bar{M}_i M_i^{-1}(D_i(\upsilon_i)\upsilon_i + C_i(\upsilon_i)\upsilon_i - \tau_{iw})$ is the collection of model uncertainties, unknown environmental disturbance. Define $f_i(\upsilon_i) = [f_{1i}, f_{2i}, f_{3i}]^T$. Since the velocity υ_i is not available, f_i cannot be directly reconstructed by RBFNN. Here, the input τ_i and output history η_i are used to reconstructed the unknown function in [22] and [33], that is

$$f_i(\upsilon_i) = W_i^T h_{ij}(\varsigma_i) + \varepsilon_i(\varsigma_i), \tag{12}$$

where $W_i \in \mathbb{R}^{m\times3}, j = 1, \ldots, m$ represent the jth hidden-layer neuron, $\varsigma_i = [\eta_i^T, \eta_i^T(t - t_d), \eta_i^T(t - 2t_d), \tau_i^T]^T$ with $t_d > 0$, $h_{ij}(\varsigma_i) \in \mathbb{R}^{m\times1}$, $||\varepsilon_i(\varsigma_i)|| \le \bar{\varepsilon}_i$, and $\bar{\varepsilon}_i$ is a positive constant.

Let $\hat{\eta}_i = [\hat{x}_i, \hat{y}_i, \hat{\psi}_i]^T$ and $\hat{\upsilon}_i = [\hat{u}_i, \hat{v}_i, \hat{r}_i]^T$ be the estimation of position η_i and velocity υ_i, respectively. Define the position estimation error as $\tilde{\eta}_i = \hat{\eta}_i - \eta_i$, and the NN based state observer is designed as

$$\dot{\hat{\eta}}_i = R_i\hat{\upsilon}_i - K_{oi1}\tilde{\eta}_i, \tag{13}$$

$$\bar{M}_i\dot{\hat{\upsilon}}_i = \tau_i - \hat{W}_i^T h_{ij}(\varsigma_i) - K_{oi2}R_i^T\tilde{\eta}_i. \tag{14}$$

where $K_{io1}, K_{io2} \in \mathbb{R}^{3\times3}$ are positive observer gain matrices to be designed.

The update law for $\hat{W}_i$ is designed as

$$\dot{\hat{W}}_i = \gamma_i h_{ij}(\varsigma_i)\tilde{\eta}_i^T R_i - \rho_i\hat{W}_i, \tag{15}$$

where $\rho_i, \gamma_i \in \mathbb{R}$ are positive constants to be designed.

Define the velocity estimation error as $\tilde{\upsilon}_i = \hat{\upsilon}_i - \upsilon_i$. Thus, the observer error dynamics can be written as

$$\dot{\tilde{\eta}}_i = R_i\tilde{\upsilon}_i - K_{io1}\tilde{\eta}_i, \tag{16}$$

$$\bar{M}_i\dot{\tilde{\upsilon}}_i = -\tilde{W}_i^T h_{ij}(\varsigma_i) + \varepsilon_i(\varsigma_i) - K_{io2}R_i{}^T\tilde{\eta}_i, \tag{17}$$

Define an observer error states as new vector $X_i = [\tilde{\eta}_i^T, \tilde{\upsilon}_i^T]^T$, and rewrite the observer error dynamics (16) and (17) as

$$\dot{X}_i = A_iX_i + B_i(-\tilde{W}_i^T h_{ij}(\varsigma_i) + \varepsilon_i(\varsigma_i)), \tag{18}$$

$$\tilde{\eta}_i = C_{oi}X_i, \tag{19}$$

where

$$A_i = \begin{bmatrix} -K_{io1} & R_i \\ -K_{io2}\bar{M}_i^{-1}R_i^T & 0_{3\times3} \end{bmatrix}, \quad B_i = \begin{bmatrix} 0_{3\times3} \\ \bar{M}_i^{-1} \end{bmatrix},$$
$$C_{oi} = [I_{3\times3}, 0_{3\times3}]. \tag{20}$$

A_i depends on nonlinear term R_i. This will make the stability analysis of designed observer difficult. Therefore, a transformation $\chi_i = T_iX_i$ with $T_i = \mathrm{diag}\{R_i^T, I_{3\times3}\}$ is introduced in [22] and [34], such that

$$\dot{\chi}_i = (A_{i0} + r_iS_T)\chi_i + B_i(-\tilde{W}_i^T h_{ij}(\varsigma_i) + \varepsilon_i(\varsigma_i)), \tag{21}$$

where $S_T = \mathrm{diag}\{S^T, 0_{3\times3}\}$ and

$$A_{i0} = \begin{bmatrix} -K_{io1} & I_{3\times3} \\ -K_{io2}\bar{M}_i^{-1} & 0_{3\times3} \end{bmatrix}. \tag{22}$$

Then the following lemma holds.

Lemma 2: The observer estimation error signal X_i is bounded, if the parameters satisfies $\frac{\rho_i}{2\gamma_i} - \frac{\bar{h}_{ij}^2}{2} > 0$ and there exist symmetric definite positive matrices $Q_i, P_i \in \mathbb{R}^{6\times6}$ such that the following inequalities satisfied

$$A_{i0}^TP_i + P_iA_{i0} + P_iB_iB_i^TP_i + Q_i + F_iF_i^T + \bar{r}_i(S_T^TP_i + P_iS_T) \le 0, \tag{23}$$

$$A_{i0}^TP_i + P_iA_{i0} + P_iB_iB_i^TP_i + Q_i + F_iF_i^T - \bar{r}_i(S_T^TP_i + P_iS_T) \le 0, \tag{24}$$

where $\bar{r}_i \in \mathbb{R}$ is the upper bound of r_i and $F_i = C_{oi}^T - P_iB_i$.

Proof: Consider the following Lyapunov function candidate as

$$V_{io} = \frac{1}{2}\chi_i^TP_i\chi_i + \frac{1}{2\gamma_i}\mathrm{tr}(\tilde{W}_i^T\tilde{W}_i) \tag{25}$$

Differentiating V_{io} with respect to time and using (15) and (21), yields

$$\begin{aligned}\dot{V}_{io} &= \chi_i^TP_i\dot{\chi} + \frac{1}{\gamma_i}\mathrm{tr}(\tilde{W}_i^T\dot{\tilde{W}}_i) \\ &= \chi_i^TP_i((A_{i0} + r_iS_T)\chi_i + B_i(-\tilde{W}_i^Th_{ij}(\varsigma_i) + \varepsilon_i(\varsigma_i))) \\ &\quad + \frac{1}{\gamma_i}\mathrm{tr}(\tilde{W}_i^T\dot{\tilde{W}}_i)\end{aligned}$$

$$\leq \chi_i^T P_i((A_{i0}+r_i S_T)\chi_i + B_i(-\tilde{W}_i^T h_{ij}(\varsigma_i)+\varepsilon_i(\varsigma_i))) + \frac{1}{\gamma_i}\mathrm{tr}(\tilde{W}_i^T\dot{\hat{W}}_i)$$
$$\leq \chi_i^T P_i(A_{i0}+r_i S_T)\chi_i - \chi_i^T F_i\tilde{W}_i^T h_{ij}(\varsigma_i) + \chi_i^T P_i B_i\varepsilon_i(\varsigma_i) - \frac{\rho_i}{\gamma_i}\mathrm{tr}(\tilde{W}_i^T\hat{W}_i). \quad (26)$$

Note that $-\mathrm{tr}(\tilde{W}_i^T\hat{W}_i) \leq -\frac{1}{2}||\tilde{W}_i||_F^2 + \frac{1}{2}||W_i||_F^2$, $-\chi_i^T F_i\tilde{W}_i^T h_{ij}(\varsigma_i) \leq \frac{1}{2}\chi_i^T F_i F_i^T\chi_i + \frac{1}{2}\tilde{W}_i^T h_{ij}(\varsigma_i)h_{ij}^T(\varsigma_i)\tilde{W}_i$, and $\chi_i^T P_i B_i\varepsilon_i(\varsigma_i) \leq \frac{1}{2}\chi_i^T P_i B_i B_i^T P_i\chi_i + \frac{1}{2}\varepsilon_i^2(\varsigma_i)$. Using (23) and (24), (26) is rewritten as

$$\dot{V}_{io} \leq -\lambda_{\min}(Q_i)\|\chi_i\|^2 - \left(\frac{\rho_i}{2\gamma_i} - \frac{\bar{h}_{ij}^2}{2}\right)\left\|\tilde{W}_i\right\|_F^2 + \frac{\rho_i}{2\gamma_i}\|W_i\|_F^2 + \frac{1}{2}\varepsilon_i^2(\varsigma_i) \leq -c_{i2}V_{io} + c_{i1}, \quad (27)$$

where $c_{i1} = \frac{\rho_i}{2\gamma_i}\|W_i\|_F^2 + \frac{1}{2}\|\bar{\varepsilon}_i(\varsigma_i)\|^2$, $c_{i2} = \min\{\frac{2\lambda_{\min}(Q_i)}{\lambda_{\max}(P_i)}, \rho_i - \gamma_i\bar{h}_{ij}^2\}$. Then, the state χ_i is bounded. Noticing $T_i^T = T_i^{-1}$, $||T_i^T|| \leq 1$ and using $X_i = T_i^T\chi_i$, the estimation error signal X_i is bounded.

B. DISTRIBUTED CONTROLLER DESIGN

Before designing the controller, an auxiliary dynamic system is constructed to handle the input constraint. The auxiliary system will guarantee the stability of the proposed distributed controller with the presence of input saturation. The auxiliary dynamic system is designed as [16]

$$\dot{\xi}_{i1} = -L_{i1}\xi_{i1} + a_{id}R_i\xi_{i2}, \quad (28)$$
$$\dot{\xi}_{i2} = -L_{i2}\xi_{i2} + \bar{M}_i^{-1}\Delta\tau_i, \quad (29)$$

where $a_{id} = d_i + a_{i0}$, $\Delta\tau_i = \tau_i - \tau_{ic}$; $\|\Delta\tau_i\| \leq \bar{\Delta}_i$, $\bar{\Delta}_i$ is an unknown positive constant, $L_{i1}, L_{i2} \in \mathbb{R}^{3\times3}$ are diagonal positive matrices to be designed, the generated auxiliary states ξ_{i1} and ξ_{i2} are used in the following distributed controller design process.

The distributed controller design process consists of two steps.

Step 1: Define the first error vector based on the communication topology and auxiliary state ξ_{i1}.

$$z_{i1} = \sum_{j\in\mathcal{N}_i} a_{ij}(\eta_i - \vartheta_i - (\eta_j - \vartheta_j)) + a_{i0}(\eta_i - \eta_d - \vartheta_i) - \xi_{i1}, \quad (30)$$

where a_{ij} and a_{i0} are defined in the Section II.

Using the MSV's dynamic (10), the time derivative of z_{i1} is given as

$$\dot{z}_{i1} = a_{id}R_i\upsilon_i - \sum_{j\in\mathcal{N}_i} a_{ij}R_j\upsilon_j - a_{i0}\dot{\eta}_d - \dot{\xi}_{i1}. \quad (31)$$

Choosing υ_i as a virtual input in (31), the *kinematic control law* α_i is proposed as

$$\alpha_i = \frac{R_i^T}{a_{id}}\{-(K_{i1} + \frac{k_{ia}}{k_{ib}^T k_{ib} - z_{i1}^T z_{i1}})z_{i1} + \sum_{j\in\mathcal{N}_i} a_{ij}R_j\hat{\upsilon}_j + a_{i0}\dot{\eta}_d - L_{i1}\xi_{i1}\}, \quad (32)$$

where $K_{i1} \in \mathbb{R}^{3\times3}$ is a positive diagonal gain matrix to be designed and $k_{ia} = \frac{3a_{id}+\theta_i}{2}$, where $\theta_i = \sum_{j\in\mathcal{N}_i} a_{ij}$. Define a compact set $\Omega_{z_{i1}} = \{|z_{i1}| < k_{ib}\}$, where k_{ib} is designed parameter.

The DSC method in [35] is introduced to avoid the calculation of the time derivative of α_i, where a first order filter was used to instead of the time derivative of α_i as $\iota_i\dot{\upsilon}_{id} = \alpha_i - \upsilon_{id}$ with time constant $\iota_i \in \mathbb{R} > 0$. However, the first order filter is sensitive to noise [36]. Therefore, a second-order LTD is used, such as

$$\begin{cases} \dot{\upsilon}_{ir} = \upsilon_{ir}^d, \\ \dot{\upsilon}_{ir}^d = -\iota_i^2(\upsilon_{ir} - a_i) - 2\iota_i\upsilon_{ir}^d. \end{cases} \quad (33)$$

Step 2: In this step, we develop a dynamic controller at the kinetic level using the LTD (33), MSV dynamic and the auxiliary state ξ_{i2}. Define the second error vector as

$$z_{i2} = \hat{\upsilon}_i - \upsilon_{ir} - \xi_{i2}. \quad (34)$$

Using (14) and (29), the time derivative of z_{i2} is derived as

$$\bar{M}_i\dot{z}_{i2} = -K_{oi2}R_i^T\tilde{\eta}_i + \tau_{ic} - \hat{W}_i^T h_{ij}(\varsigma_i) - \bar{M}_i(\dot{\upsilon}_{ir} - L_{i2}\xi_{i2}). \quad (35)$$

To stabilize z_{i2}, a *kinetic control law* is designed as

$$\tau_{ic} = -K_{i2}z_{i2} + \bar{M}_i(\upsilon_{ir}^d - L_{i2}\xi_{i2}) + \hat{W}_i^T h_{ij}(\varsigma_i), \quad (36)$$

where $K_{i2} \in \mathbb{R}^{3\times3}$ is positive diagonal matrix to be designed and $\hat{W}_i^T h_{ij}(\varsigma_i)$ is the estimation of $f_i(\upsilon_i)$.

Substituting (32) and (36) into (31) and (35), respectively, the time derivative of z_{i1} and z_{i2} can be rewritten as

$$\dot{z}_{i1} = -(K_{i1} + \frac{k_{ia}}{k_{ib}^T k_{ib} - z_{i1}^T z_{i1}})z_{i1} + a_{id}R_i(-\tilde{\upsilon}_i + z_{i2} + q_i) + \theta_i R_j\tilde{\upsilon}_j. \quad (37)$$
$$\bar{M}_i\dot{z}_{i2} = -K_{i2}z_{i2} - K_{oi2}R_i^T\tilde{\eta}_i, \quad (38)$$

where $q_i = \upsilon_{ir} - \alpha_i$.

The following theorem is given to point out the stability of overall closed-loop system.

Theorem 1: Consider the network system consisting of the MSV dynamics (5), (6), the distributed control law (36), the observer (13) and (14), the NN update law (15) and the auxiliary dynamic system (28) and (29) with unknown environmental disturbances and input saturation under assumption 1-3. Then, the proposed neuroadaptive distributed output feedback control scheme guarantees: 1) All signals in the closed-loop system are bounded. 2) All follower MSVs are able to track the reference signal with a bounded tracking error. 3) The output position of each MSV satisfies the output constraint.

Proof: Choose a Lyapunov function candidate as follows

$$V_1 = \frac{1}{2}\sum_{i=1}^{n}\{2V_{io} + \ln\frac{k_{ib}^T k_{ib}}{k_{ib}^T k_{ib} - z_{i1}^T z_{i1}} + z_{i2}^T\bar{M}_i z_{i2} + \xi_{i1}^T\xi_{i1} + \xi_{i2}^T\xi_{i2}\}, \quad (39)$$

By using the BLF $\ln \frac{k_{ib}^T k_{ib}}{k_{ib}^T k_{ib} - z_{i1}^T z_{i1}}$, we can guarantee that the output constraint for each vessel are satisfied. The time derivative of (39) is

$$\dot{V}_1 = \sum_{i=1}^{n} \{\dot{V}_{io} + \frac{z_{i1}^T \dot{z}_{i1}}{k_{ib}^T k_{ib} - z_{i1}^T z_{i1}} + z_{i2}^T \bar{M}_i \dot{z}_{i2} + \xi_{i1}^T \dot{\xi}_{i1} + \xi_{i2}^T \dot{\xi}_{i2}\}. \tag{40}$$

Similar to [16], it can prove that q_i is bounded. Let $\bar{q}_i$ be the upper bound of q_i. Using Young's inequality, the inequalities $\frac{-z_{i1}^T R_i \tilde{\upsilon}_i}{k_{ib}^T k_{ib} - z_{i1}^T z_{i1}} \leq \frac{z_{i1}^T z_{i1}}{2(k_{ib}^T k_{ib} - z_{i1}^T z_{i1})^2} + \frac{1}{2}\tilde{\upsilon}_i^T \tilde{\upsilon}_i$, $\frac{z_{i1}^T R_i z_{i2}}{k_{ib}^T k_{ib} - z_{i1}^T z_{i1}} \leq \frac{z_{i1}^T z_{i1}}{2(k_{ib}^T k_{ib} - z_{i1}^T z_{i1})^2} + \frac{1}{2} z_{i2}^T z_{i2}$, $\frac{z_{i1}^T R_i q_i}{k_{ib}^T k_{ib} - z_{i1}^T z_{i1}} \leq \frac{z_{i1}^T z_{i1}}{2(k_{ib}^T k_{ib} - z_{i1}^T z_{i1})^2} + \frac{1}{2}\|\bar{q}_i\|^2$, $\frac{z_{i1}^T R_j \tilde{\upsilon}_j}{k_{ib}^T k_{ib} - z_{i1}^T z_{i1}} \leq \frac{z_{i1}^T z_{i1}}{2(k_{ib}^T k_{ib} - z_{i1}^T z_{i1})^2} + \frac{1}{2}\tilde{\upsilon}_j^T \tilde{\upsilon}_j$, $-z_{i2}^T K_{io2} R_i^T \tilde{\eta}_i \leq \frac{\lambda_{\max}(K_{io2})}{2} z_{i2}^T z_{i2} + \frac{\lambda_{\max}(K_{io2})}{2} \tilde{\eta}_i^T \tilde{\eta}_i$, $\xi_{i1}^T R_i \xi_{i2} \leq \frac{1}{2}\xi_{i1}^T \xi_{i1} + \frac{1}{2}\xi_{i2}^T \xi_{i2}$ and $\xi_{i2}^T \bar{M}_i^{-1} \Delta_{\tau_i} \leq \frac{\lambda_{\max}(\bar{M}_i^{-1})}{2} \xi_{i2}^T \xi_{i2} + \frac{\lambda_{\max}(\bar{M}_i^{-1})}{2} \|\bar{\Delta}_i\|^2$ hold. According to Lemma 1, yields

$$\begin{aligned}
\dot{V}_1 \leq \sum_{i=1}^{n} \{ & \dot{V}_{io} - \lambda_{\min}(K_{i1}) \ln \frac{k_{ib}^T k_{ib}}{k_{ib}^T k_{ib} - z_{i1}^T z_{i1}} \\
& - (\lambda_{\min}(K_{i2}) - \frac{a_{id} + \lambda_{\max}(K_{io2})}{2}) z_{i2}^T z_{i2} \\
& - (\lambda_{\min}(L_{i1}) - \frac{a_{id}}{2}) \xi_{i1}^T \xi_{i1} - (\lambda_{\min}(L_{i2}) - \frac{a_{id}}{2} \\
& - \frac{\lambda_{\max}(\bar{M}_i^{-1})}{2}) \xi_{i2}^T \xi_{i2} + \frac{\lambda_{\max}(K_{io2})}{2} \tilde{\eta}_i^T \tilde{\eta}_i \\
& + \frac{a_{id} + \theta_i}{2} \tilde{\upsilon}_i^T \tilde{\upsilon}_i + \frac{a_{id}}{2} \|\bar{q}_i\|^2 + \frac{\lambda_{\max}(\bar{M}_i^{-1})}{2} \|\bar{\Delta}_i\|^2 \}.
\end{aligned} \tag{41}$$

Let $l_{i1} = \lambda_{\min}(K_{i1})$, $l_{i2} = \lambda_{\min}(K_{i2}) - \frac{a_{id} + \lambda_{\max}(K_{io2})}{2}$, $l_{i3} = \lambda_{\min}(L_{i1}) - \frac{a_{id}}{2}$, $l_{i4} = \lambda_{\min}(L_{i2}) - \frac{a_{id}}{2} - \frac{\lambda_{\max}(\bar{M}_i^{-1})}{2}$ and $c_{i3} = \frac{a_{id}}{2}\|\bar{q}_i\|^2 + \frac{\lambda_{\max}(\bar{M}_i^{-1})}{2}\|\bar{\Delta}_i\|^2$. Using $\chi_i = T_i X_i$, the inequality (41) becomes

$$\begin{aligned}
\dot{V}_1 \leq \sum_{i=1}^{n} \{ & \dot{V}_{io} - l_{i1} \ln \frac{k_{ib}^T k_{ib}}{k_{ib}^T k_{ib} - z_{i1}^T z_{i1}} - l_{i2} \|z_{i2}\|^2 \\
& - l_{i3} \|\xi_{i1}\|^2 - l_{i4} \|\xi_{i2}\|^2 + \lambda_{\max}(A_{i1}) \|\chi_i\|^2 + c_{i3}\},
\end{aligned} \tag{42}$$

where $A_{i1} = \mathrm{diag}\{\frac{\lambda_{\max}(K_{io2})}{2}, \frac{a_{id} + \theta_i}{2}\}$. Substituting (27) into (42), leads to

$$\begin{aligned}
\dot{V}_1 & \leq \sum_{i=1}^{n} \{-c_{i2} V_{io} - l_{i1} \ln \frac{k_{ib}^T k_{ib}}{k_{ib}^T k_{ib} - z_{i1}^T z_{i1}} - l_{i2} \|z_{i2}\|^2 \\
& \quad - l_{i3} \|\xi_{i1}\|^2 - l_{i4} \|\xi_{i3}\|^2 + \lambda_{\max}(A_{i1}) \|\chi_i\|^2 \\
& \quad + c_{i1} + c_{i3}\} \\
& \leq \sum_{i=1}^{n} \{-(c_{i2} - \frac{\lambda_{\max}(A_{i1})}{\lambda_{\min}(P_i)}) V_{io} - l_{i1} \ln \frac{k_{ib}^T k_{ib}}{k_{ib}^T k_{ib} - z_{i1}^T z_{i1}} \\
& \quad - l_{i2} \|z_{i2}\|^2 - l_{i3} \|\xi_{i1}\|^2 - l_{i4} \|\xi_{i3}\|^2 + c_{i1} + c_{i3}\} \\
& \leq -c_{i4} V_1 + c_{i5},
\end{aligned} \tag{43}$$

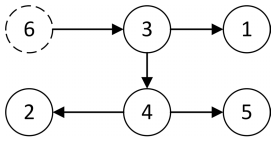

FIGURE 2. Communication topology.

where $c_{i4} = \min\{c_{i2} - \frac{\lambda_{\max}(A_{i1})}{\lambda_{\min}(P_i)}, 2l_{i1}, \frac{2l_{i2}}{\lambda_{\max}(\bar{M}_i)}, 2l_{i3}, 2l_{i4}\} > 0$ and $c_{i5} = \sum_{i=1}^{n}\{c_{i1} + c_{i3}\}$.

From the definition of V_1, it can conclude that χ_i, $\tilde{W}_i$, z_{i2}, ξ_{i1}, ξ_{i2} and $\ln \frac{k_{ib}^T k_{ib}}{k_{ib}^T k_{ib} - z_{i1}^T z_{i1}}$ are bounded, where $\ln \frac{k_{ib}^T k_{ib}}{k_{ib}^T k_{ib} - z_{i1}^T z_{i1}}$ implies z_{i1} always remain in the set $\Omega_{z_{ii}}$, only if the initial values are $z_{i1}(0)$ remains in the set $\Omega_{z_{i1}}$. Therefore, all signals in the closed-loop are bounded.

Define the absolute tracking error in earth-fixed frame as $e_i = \eta_i - \vartheta_i - \eta_d$. From (30), we have $z_1 + \xi_1 = (H \otimes I_3)e$, where $\mathcal{H}$ is defined in the section II, $e = [e_1^T, \ldots, e_n^T]^T$, $z_1 = [z_{11}^T, \ldots, z_{n1}^T]^T$ and $\xi_1 = [\xi_{11}^T, \ldots, \xi_{n1}^T]^T$. Then, the following inequality holds $\|e\| \leq \frac{\|z_1\| + \|\xi_1\|}{\underline{o}(\mathcal{H})}$, where $\underline{o}(\mathcal{H})$ denotes the minimal singular value of $\mathcal{H}$. Then, $\|e\|$ is bounded.

According to Lemma 1, $|z_{i1}| < k_{ib}$ holds. From assumption 4, $|\eta_d| \leq \bar{\eta}_d$ with $\bar{\eta}_d$ being a positive constant. Using $\|e\| \leq \frac{\|z_1\| + \|\xi_1\|}{\underline{o}(\mathcal{H})}$ and $e_i = \eta_i - \vartheta_i - \eta_d \leq k_{ib} + \bar{\xi}_{i1}$, then $|\eta_i - \vartheta_i| < \frac{k_{ib} + \bar{\xi}_{i1}}{\underline{o}(\mathcal{H})} + \bar{\eta}_d$ holds, where $\xi_i \leq \sqrt{c_{i4}/l_{i3}} = \bar{\xi}_{i1}$. Define $k_{ic} = \frac{k_{ib} + \bar{\xi}_{i1}}{\underline{o}(\mathcal{H})} + \bar{\eta}_d$, then $|\eta_i - \vartheta_i| < k_{ic}$, which means the output constraint for each vessel is satisfied the set Ω_{η_i}.

This completes the proof.

IV. SIMULATION RESULTS

In this section, numerical simulation and comparison study are given to show the effectiveness of the proposed neuroadaptive distributed output feedback control strategy. We consider a virtual leader (the reference signal $\eta_d = [x_d, y_d, \psi_d]^T$) indexed by 6 and five follower MSVs indexed by 1, 2, 3, 4, 5, respectively. The directed communication topology is shown in Figure 2. In simulations, the model of surface ship Cybership II is used [37]. The time-varying environmental disturbances are modeled as $\tau_{iw} = R_i^T b_i$ with the first-order Markov process $\dot{b}_{iw} + \Psi_{iw} b_{iw} = w_i$, where $\Psi_{iw} \in \mathbb{R}^{3\times3}$ is positive constant and $w_i \in \mathbb{R}^3$ is Gaussian white noise.

A. SIMULATION OF PROPOSED CONTROLLER

The desired reference trajectory signal is given in (44). The initial position of MSVs are chosen as $\eta_1 = [-1.4\text{m}, 0.2\text{m}, \frac{\pi}{4}\text{rad}]^T$, $\eta_2 = [0.1\text{m}, 1\text{m}, \frac{\pi}{4}\text{rad}]^T$, $\eta_3 = [0.2\text{m}, 0.1\text{m}, \frac{\pi}{4}\text{rad}]^T$, $\eta_4 = [-1.3\text{m}, 0.2\text{m}, \frac{\pi}{4}\text{rad}]^T$, and $\eta_5 = [0.1\text{m}, -1.5\text{m}, \frac{\pi}{4}\text{rad}]^T$, respectively. The desired deviation of vessels are set as $\vartheta_1 = [1.2\text{m}, 0\text{m}, 0\text{rad}]^T$, $\vartheta_2 = [0\text{m}, 1.2\text{m}, 0\text{rad}]^T$, $\vartheta_3 = [0\text{m}, 0\text{m}, 0\text{rad}]^T$, $\vartheta_4 = [-1.2\text{m}, 0\text{m}, 0\text{rad}]^T$, and $\vartheta_5 = [0\text{m}, -1.2\text{m}, 0\text{rad}]^T$, respectively. The initial position and velocity estimation values of vessels are set as

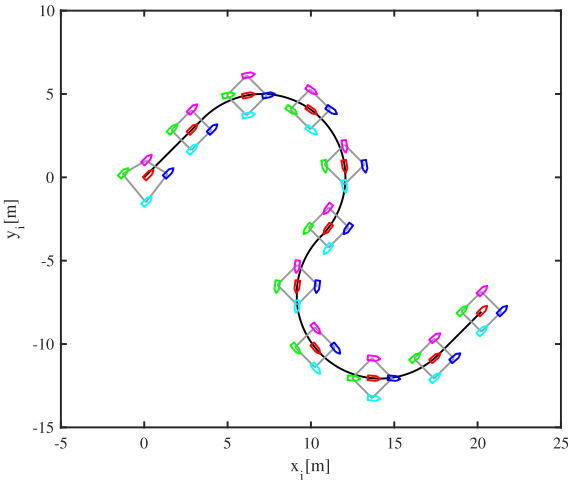

FIGURE 3. Formation tracking control using the proposed controller.

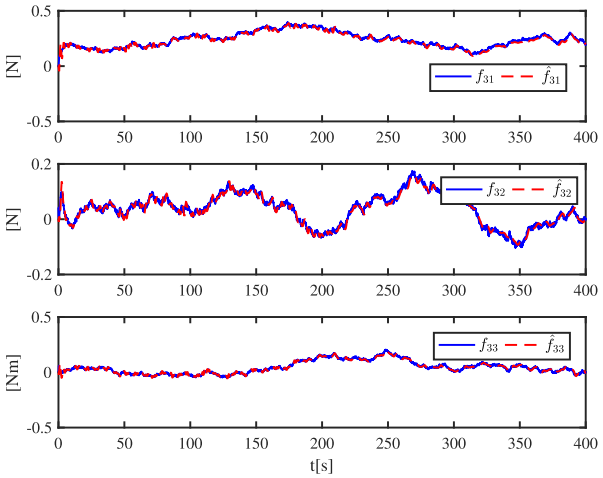

FIGURE 4. Unknown function and RBFNN estimation of MSV 3.

$\hat{\eta}_i(0) = \eta_i(0)$ and $\hat{v}_i(0) = [0\text{m/s}, 0\text{m/s}, 0\text{rad/s}]^T$. The control forces and moment are constrained as $\tau_{i1\,\max} = -\tau_{i1\,\min} = 2\text{N}$, $\tau_{i2\,\max} = -\tau_{i2\,\min} = 2\text{N}$ and $\tau_{i3\,\max} = -\tau_{i3\,\min} = 1.5\text{Nm}$. The constraint k_{ib} is set as $k_{ib} = [0.5\text{m}, 0.6\text{m}, 0.15\text{rad}]$.

$$\begin{cases} [\frac{t}{10}\cos(\frac{\pi}{4}), \frac{t}{10}\sin(\frac{\pi}{4}), \frac{\pi}{4}], \\ \qquad 0 \le t < 50; \\ \left[5\cos(\frac{3\pi}{4} - \frac{1}{50}(t-50)) + 10\cos(\frac{\pi}{4}), \right. \\ \left. 5\sin(\frac{3\pi}{4} - \frac{1}{50}(t-50)), \frac{1}{50}(t-50) + \frac{\pi}{4}\right], \\ \qquad 50 \le t < 50 + 50\pi; \\ \left[5\cos(\frac{3\pi}{4} + \frac{1}{50}(t-50-50\pi)) + 20\cos(\frac{\pi}{4}), \right. \\ 5\sin(\frac{3\pi}{4} + \frac{1}{50}(t-50-50\pi)) - 10\sin(\frac{\pi}{4}), \\ \left. \frac{1}{50}(t-50-50\pi) - \frac{3\pi}{4}\right], \\ \qquad 50 + 50\pi \le t < 50 + 100\pi; \\ [25\cos(\frac{\pi}{4}) + \frac{t-50-100\pi}{10}\cos(\frac{\pi}{4}), \\ -15\sin(\frac{\pi}{4}) + \frac{t-50-100\pi}{10}\sin(\frac{\pi}{4}), \frac{\pi}{4}], \\ \qquad t \ge 50 + 100\pi; \end{cases} \tag{44}$$

The observer for each MSV is designed as (13) and (14), the parameters of designed observer are chosen as $K_{io1} = 30 \times \text{diag}\{1, 1, 1\}$, $K_{io2} = 30 \times \text{diag}\{1, 1, 1\}$.The controller for each vessel is designed as (36), the auxiliary system is designed as (28) and (29). The parameters are selected as $K_{i1} = 2.2 \times \text{diag}\{1, 1, 1\}$, $K_{i2} = \text{diag}\{60, 60, 23\}$, $\iota_i = 10$, $L_{i1} = 0.6 \times \text{diag}\{1, 1, 1\}$, and $L_{i2} = 1.2 \times \text{diag}\{1, 1, 1\}$. The RBFNN with nine neurons in the hidden layer is used. The update law for $\hat{W}_i$ is designed as (15). The parameters are selected as $\gamma_i = 1000$ and $\rho_i = 0.2$.

The simulation results are illustrated from Figure 3 to Figure 7. Figure 3 demonstrates the formation tracking

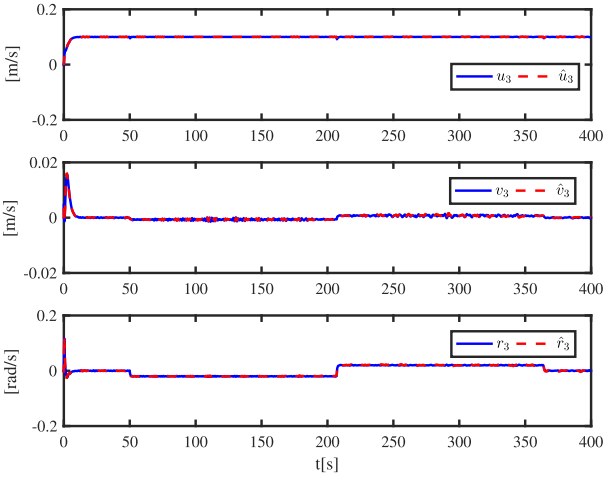

FIGURE 5. Velocity estimation of MSV 3.

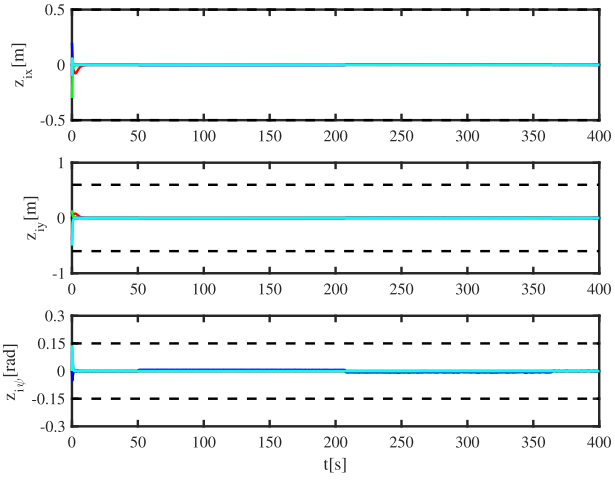

FIGURE 6. Tracking errors of five MSVs under the proposed controller.

control of five MSVs, in which one can see that all the MSVs are able to track the desired signal with desired formation successfully. The performance of RBFNN approximating

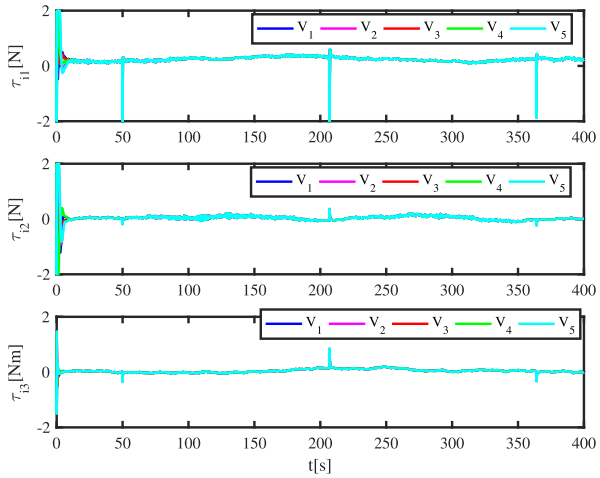

FIGURE 7. Control inputs of five MSVs under the proposed controller.

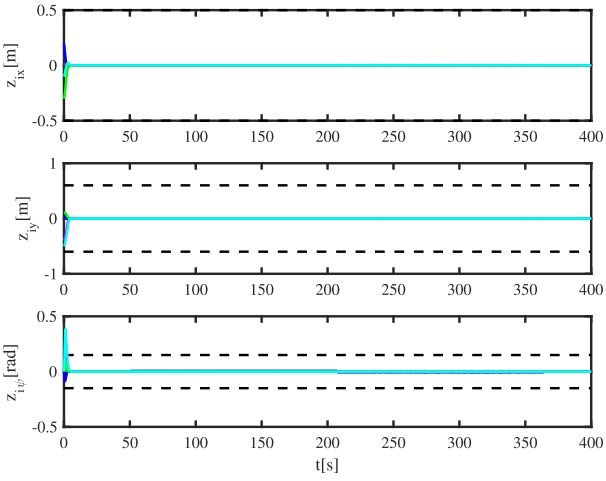

FIGURE 8. Tracking errors of five MSVs under the NDSC based controller.

of MSV 3 is shown in Figure 4. It can be seen that the lumped unknown model dynamics and environmental disturbances function can be identified by the proposed observer. Figure 5 depicts that the velocity estimation of MSV 3 is also nicely reconstructed using proposed observer. In Figure 6, even if there are initial deviations, the formation tracking error converge to a small neighborhood around zero without violating the imposed constraint. Figure 7 shows that the control inputs of five MSVs are bounded by saturation, where the sudden changes of the control forces after 50s are caused by the switching of the trajectories.

B. COMPARISON STUDY

In order to further evaluate the performance of the proposed control scheme, a neuroadaptive DSC (NDSC) based distributed output feedback tracking controller without auxiliary dynamic system is carried out. The NDSC based method is

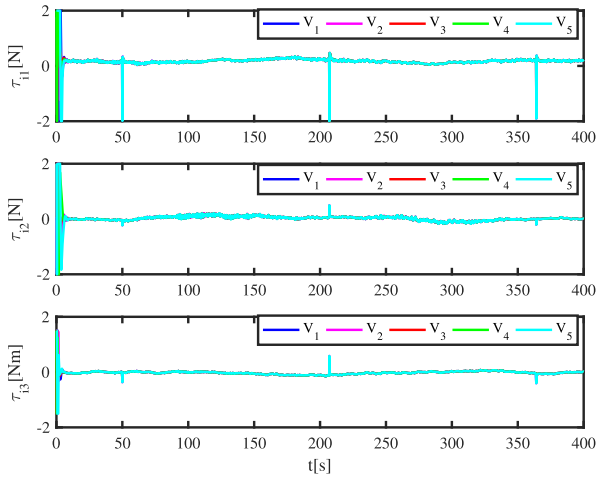

FIGURE 9. Control inputs of five MSVs under the NDSC based controller.

given by

$$\begin{cases} z_{i1} = \sum_{j\in N_i} a_{ij}(\eta_i - \vartheta_i - (\eta_j - \vartheta_j)) + a_{i0}(\eta_i - \eta_d - \vartheta_i) \\ \alpha_i = \dfrac{R^T}{a_{id}}\{-K_{i1}z_{i1} + \sum_{j\in N_i} a_{ij}R_j\hat{\upsilon}_j + a_{i0}\dot{\eta}_d\} \\ \dot{\upsilon}_{ir} = -\iota_i^2(\upsilon_{ir} - \alpha_i) \\ z_{i2} = \hat{\upsilon}_i - \upsilon_{ir} \\ \tau_{ic} = -K_{i2}z_{i2} + \bar{M}_i\dot{\upsilon}_{ir} + \hat{W}_i^T h_{ij}(\varsigma_i) \end{cases} \tag{45}$$

where the control parameters are chosen as same as proposed controller. The simulation results are shown as Figure 8 and 9. Comparing Figure 6 and Figure 8, it is clear that the tracking error of proposed control scheme stays in desired constrained region. However, the yaw constraints of the NDSC based controller is violated in the first 10s. Comparing Figure 7 and Figure 9, the control forces are much larger and more oscillations using the NDSC based controller than the proposed controller in the first 10s.

V. CONCLUSION

In this paper, we address the distributed output feedback formation tracking control for multiple MSVs in the presence of model uncertainties, unknown environmental disturbances, and input and output constraints. Neuroadaptive observer is proposed such that the unmeasured velocity and unknown model dynamics can be simultaneously estimated. The distributed output controller is designed based on the auxiliary system, LTD, BLF and the estimation velocity of neighboring MSVs. With the proposed scheme, it is proved that all error signals in the closed-loop are bounded. Simulation and comparison results verify the tracking performance of the proposed distributed controller. For the future work, it is of interest to develop formation tracking control for underactuated marine surface vessels.

REFERENCES

[1] P. Mahacek, C. A. Kitts, and I. Mas, "Dynamic guarding of marine assets through cluster control of automated surface vessel fleets," *IEEE/ASME Trans. Mechatronics*, vol. 17, no. 1, pp. 65–75, Feb. 2012.
[2] P. I. B. Berntsena, O. M. Aamob, B. J. Leiraa, and A. J. Sørensen, "Structural reliability-based control of moored interconnected structures," *Control Eng. Pract.*, vol. 16, no. 4, pp. 495–504, 2009.
[3] G. Xia, X. Shao, and A. Zhao, "Robust nonlinear observer and observer-backstepping control design for surface ships," *Asian J. Control*, vol. 17, no. 4, pp. 1377–1393, 2015.
[4] Z. R. Ren, R. Skjetne, Z. Y. Jiang, Z. Gao, and A. S. Verma, "Integrated GNSS/IMU hub motion estimator for offshore wind turbine blade installation," *Mech. Syst. Signal Process.*, vol. 123, pp. 222–243, May 2019.
[5] I. F. Ihle, R. Skjetne, and T. I. Fossen, "Output feedback control for maneuvering systems using observer backstepping," in *Proc. IEEE Int. Symp., Mediterrean Conf. Control Automat. Intell. Control*, Jun. 2005, pp. 1512–1517.
[6] S. S. Ge, C. C. Hang, and T. Zhang, "Adaptive neural network control of nonlinear systems by state and output feedback," *IEEE Trans. Syst., Man, Cybern. B, Cybern.*, vol. 29, no. 6, pp. 818–828, Dec. 1999.
[7] G. Xia, H. Wu, and X. Shao, "Adaptive filtering backstepping for ships steering control without velocity measurements and with input constraints," *Math. Problems Eng.*, vol. 2014, Mar. 2014, Art. no. 218585.
[8] G. Wen, S. S. Ge, C. L. P. Chen, F. Tu, and S. Wang, "Adaptive tracking control of surface vessel using optimized backstepping technique," *IEEE Trans. Cybern.*, vol. 49, no. 9, pp. 3420–3431, Sep. 2019.
[9] J. Du, X. Hu, H. Liu, and C. L. P. Chen, "Adaptive robust output feedback control for a marine dynamic positioning system based on a high-gain observer," *IEEE Trans. Neural Netw. Learn. Syst.*, vol. 26, no. 11, pp. 2775–2786, Nov. 2015.
[10] L.-J. Zhang, H.-M. Jia, and X. Qi, "NNFFC-adaptive output feedback trajectory tracking control for a surface ship at high speed," *Ocean Eng.*, vol. 38, no. 13, pp. 1430–1438, 2011.
[11] Z. Peng, D. Wang, H. H. Liu, G. Sun, and H. Wang, "Distributed robust state and output feedback controller designs for rendezvous of networked autonomous surface vehicles using neural networks," *Neurocomputing*, vol. 115, pp. 130–141, Sep. 2013.
[12] K. P. Tee and S. S. Ge, "Control of fully actuated ocean surface vessels using a class of feedforward approximators," *IEEE Trans. Control Syst. Technol.*, vol. 14, no. 4, pp. 750–756, Jul. 2006.
[13] C. Wen, J. Zhou, Z. Liu, and H. Su, "Robust adaptive control of uncertain nonlinear systems in the presence of input saturation and external disturbance," *IEEE Trans. Autom. Control*, vol. 56, no. 7, pp. 1672–1678, Jul. 2011.
[14] M. Chen, S. S. Ge, and B. Ren, "Adaptive tracking control of uncertain MIMO nonlinear systems with input constraints," *Automatica*, vol. 47, no. 3, pp. 452–465, Mar. 2011.
[15] H. Wang, D. Wang, and Z. Peng, "Adaptive dynamic surface control for cooperative path following of marine surface vehicles with input saturation," *Nonlinear Dyn.*, vol. 77, no. 1, pp. 107–117, Feb. 2014.
[16] G. Xia, C. Sun, B. Zhao, and J. Xue, "Cooperative control of multiple dynamic positioning vessels with input saturation based on finite-time disturbance observer," *Int. J. Control, Autom. Syst.*, vol. 17, no. 2, pp. 370–379, Feb. 2019.
[17] I. A. F. Ihle, J. Jouffroy, and T. I. Fossen, "Formation control of marine surface craft: A lagrangian approach," *IEEE J. Ocean. Eng.*, vol. 31, no. 4, pp. 922–934, Oct. 2006.
[18] T. Keviczky, F. Borrelli, K. Fregene, D. Godbole, and G. J. Balas, "Decentralized receding horizon control and coordination of autonomous vehicle formations," *IEEE Trans. Control Syst. Technol.*, vol. 16, no. 1, pp. 19–33, Jan. 2008.
[19] L. Chen, J. J. Hopman, and R. R. Negenborn, "Distributed model predictive control for vessel train formations of cooperative multi-vessel systems," *Transp. Res. C, Emerg. Technol.*, vol. 92, pp. 101–118, Jul. 2018.
[20] M. Zhu and S. Martinez, "On distributed constrained formation control in operator–vehicle adversarial networks," *Automatica*, vol. 49, no. 12, pp. 3571–3582, 2013.
[21] Z. Peng, J. Wang, and D. Wang, "Containment maneuvering of marine surface vehicles with multiple parameterized paths via spatial-temporal decoupling," *IEEE/ASME Trans. Mechatronics*, vol. 22, no. 2, pp. 1026–1036, Apr. 2017.
[22] Z. Peng, J. Wang, and D. Wang, "Distributed containment maneuvering of multiple marine vessels via neurodynamics-based output feedback," *IEEE Trans. Ind. Electron.*, vol. 64, no. 5, pp. 3831–3839, May 2017.
[23] J. Mei, W. Ren, and G. Ma, "Distributed containment control for Lagrangian networks with parametric uncertainties under a directed graph," *Automatica*, vol. 48, no. 4, pp. 653–659, Apr. 2012.
[24] H. Liu, L. Cheng, M. Tan, and Z.-G. Hou, "Containment control of continuous-time linear multi-agent systems with aperiodic sampling," *Automatica*, vol. 57, pp. 78–84, Jul. 2015.
[25] B. Ren, S. S. Ge, K. P. Tee, and T. H. Lee, "Adaptive neural control for output feedback nonlinear systems using a barrier Lyapunov function," *IEEE Trans. Neural Netw.*, vol. 21, no. 8, pp. 1339–1345, Aug. 2010.
[26] G. Xia, J. Xue, C. Sun, and B. Zhao, "Backstepping control using Barrier Lyapunov function for dynamic positioning control system with passive observer," *Math. Problems Eng.*, vol. 2019, Feb. 2019, Art. no. 8709369.
[27] W. He, Z. Yin, and C. Sun, "Adaptive neural network control of a marine vessel with constraints using the asymmetric barrier Lyapunov function," *IEEE Trans. Cybern.*, vol. 47, no. 7, pp. 1641–1651, Jul. 2017.
[28] Z. Zheng, Y. Huang, L. Xie, and B. Zhu, "Adaptive trajectory tracking control of a fully actuated surface vessel with asymmetrically constrained input and output," *IEEE Trans. Control Syst. Technol.*, vol. 26, no. 5, pp. 1851–1859, Sep. 2018.
[29] J. Sun and C. Liu, "Distributed zero-sum differential game for multi-agent systems in strict-feedback form with input saturation and output constraint," *Neural Netw.*, vol. 106, pp. 8–19, Oct. 2018.
[30] X. Cai, C. Wang, G. Wang, and D. Liang, "Distributed consensus control for second-order nonlinear multi-agent systems with unknown control directions and position constraints," *Neurocomputing*, vol. 306, pp. 61–67, Sep. 2018.
[31] S. Seshagiri and H. K. Khalil, "Output feedback control of nonlinear systems using RBF neural networks," *IEEE Trans. Neural Netw.*, vol. 11, no. 1, pp. 69–79, Jan. 2000.
[32] T. I. Fossen, *Marine Control Systems Guidance, Navigation, and Control of Ships, Rigs and Underwater Vehicles*, 1st ed. Trondheim, Norway: Marine Cybernetics, 2002.
[33] A. J. Calise, N. Hovakimyan, and M. Idan, "Adaptive output feedback control of nonlinear systems using neural networks," *Automatica*, vol. 37, no. 8, pp. 1201–1211, Aug. 2001.
[34] S. A. Værnø, A. H. Brodtkorb, R. Skjetne, and V. Calabrò, "Time-varying model-based observer for marine surface vessels in dynamic positioning," *IEEE Access*, vol. 5, pp. 14787–14796, 2017.
[35] D. Swaroop, J. K. Hedrick, P. P. Yip, and J. C. Gerdes, "Dynamic surface control for a class of nonlinear systems," *IEEE Trans. Autom. Control*, vol. 45, no. 10, pp. 1893–1899, Oct. 2000.
[36] B.-Z. Guo and Z.-L. Zhao, "Active disturbance rejection control: Theoretical perspectives," *Commun. Inf. Syst.*, vol. 15, no. 3, pp. 361–421, 2015.
[37] R. Skjetne, T. I. Fossen, and P. V. Kokotović, "Adaptive maneuvering, with experiments, for a model ship in a marine control laboratory," *Automatica*, vol. 41, no. 2, pp. 289–298, 2005.

GUOQING XIA received the Ph.D. degree in control theory and control engineering from Harbin Engineering University (HEU), in 2001, where he is currently a Professor. His research interests include ship dynamic positioning control technique, intelligent control theory, and system simulation technique.

CHUANG SUN received the bachelor's degree in automation from the Anyang Institute of Technology, in 2015. He is currently pursuing the Ph.D. degree in control science and engineering with Harbin Engineering University. His research interests include ship motion control, cooperative control, and nonlinear control theory.

BO ZHAO received the bachelor's degree in automation and the master's degree in navigation, guidance, and control from the Beijing University of Aeronautics and Astronautics (BUAA), in 2006 and 2009, respectively, and the Ph.D. degree in marine cybernetics from the Norwegian University of Science and Technology, in 2015. From 2013 to 2018, he served as a Senior Marine System Advisor for Global Maritime, where he developed hardware-in-the-loop testing for dynamic positioning systems. He is currently an Associate Professor with Harbin Engineering University. His research interests include applying advanced control and artificial intelligence in the control of vessel, underwater robotics, and other marine systems.

XIAOMING XIA received the bachelor's degree in automation from the Luoyang Institute of Science and Technology, in 2016. He is currently pursuing the Ph.D. degree in control science and engineering with Harbin Engineering University. His research interests include ship motion control, intelligent control theory, and multiagent systems.

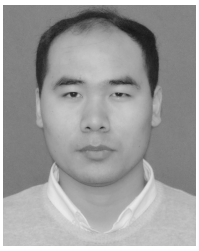

XIANXIN SUN received the bachelor's degree in automation from Yantai University, in 2014, and the master's degree in navigation, guidance, and control from the Guilin University of Electronic Technology, in 2017. He is currently pursuing the Ph.D. degree in control science and engineering with Harbin Engineering University. His research interests include thrust allocation and ship motion control.